

Laplacian-level density functionals for the kinetic energy density and exchange-correlation energy

John P. Perdew and Lucian A. Constantin*

Quantum Theory Group, Department of Physics, Tulane University, New Orleans, Louisiana 70118, USA
(Received 16 December 2006; revised manuscript received 14 February 2007; published 19 April 2007)

We construct a Laplacian-level meta-generalized-gradient-approximation (meta-GGA) for the noninteracting (Kohn-Sham orbital) positive kinetic energy density τ of an electronic ground state of density n . This meta-GGA is designed to recover the fourth-order gradient expansion τ^{GE4} in the appropriate slowly varying limit and the von Weizsäcker expression $\tau^W = |\nabla n|^2 / (8n)$ in the rapidly varying limit. It is constrained to satisfy the rigorous lower bound $\tau^W(\mathbf{r}) \leq \tau(\mathbf{r})$. Our meta-GGA is typically a strong improvement over the gradient expansion of τ for atoms, spherical jellium clusters, jellium surfaces, the Airy gas, Hooke's atom, one-electron Gaussian density, quasi-two-dimensional electron gas, and nonuniformly scaled hydrogen atom. We also construct a Laplacian-level meta-GGA for exchange and correlation by employing our approximate τ in the Tao-Perdew-Staroverov-Scuseria (TPSS) meta-GGA density functional. The Laplacian-level TPSS gives almost the same exchange-correlation enhancement factors and energies as the full TPSS, suggesting that τ and $\nabla^2 n$ carry about the same information beyond that carried by n and ∇n . Our kinetic energy density integrates to an orbital-free kinetic energy functional that is about as accurate as the fourth-order gradient expansion for many real densities (with noticeable improvement in molecular atomization energies), but considerably more accurate for rapidly varying ones.

DOI: [10.1103/PhysRevB.75.155109](https://doi.org/10.1103/PhysRevB.75.155109)

PACS number(s): 71.15.Mb, 31.15.Ew

I. INTRODUCTION

In ground-state density-functional theory, the noninteracting kinetic energy (KE) T_s of a system of N electrons may be treated as an exact functional of the occupied Kohn-Sham¹ (KS) orbitals $\{\phi_i\}$, and only the exchange-correlation energy has to be approximated. However, finding an accurate orbital-free KE functional² will simplify and speed up by orders of magnitude any KS self-consistent calculation. In general, a kinetic energy density (KED) is any function which integrates to the noninteracting kinetic energy T_s :

$$T_s[n_\uparrow, n_\downarrow] = \int d\mathbf{r} \tau, \quad (1)$$

where $n_\uparrow(\mathbf{r})$ and $n_\downarrow(\mathbf{r})$ are the electron-spin densities and $\tau(\mathbf{r}) = \tau_\uparrow([n_\uparrow], \mathbf{r}) + \tau_\downarrow([n_\downarrow], \mathbf{r})$. Because of the local version of the spin-scaling relation³

$$\tau_\sigma([n_\sigma], \mathbf{r}) = (1/2)\tau([n = 2n_\sigma], \mathbf{r}), \quad (2)$$

we will only need to show our expressions for spin-unpolarized systems with $n_\uparrow = n_\downarrow = n/2$. Like other energy densities, the KED is not unique. There are two important forms of the KED: one which depends on the Laplacian of the Kohn-Sham orbitals and follows directly from the Kohn-Sham self-consistent equations:

$$\tau^L(\mathbf{r}) = - \left(\frac{1}{2} \right) \sum_{i=1}^N \phi_i^*(\mathbf{r}) \nabla^2 \phi_i(\mathbf{r}), \quad (3)$$

and another which is positive definite:

$$\tau(\mathbf{r}) = \left(\frac{1}{2} \right) \sum_{i=1}^N |\nabla \phi_i(\mathbf{r})|^2 = \tau^L(\mathbf{r}) + \frac{1}{4} \nabla^2 n(\mathbf{r}), \quad (4)$$

where $n(\mathbf{r}) = \sum_{i=1}^N |\phi_i(\mathbf{r})|^2$ is the electronic density. (We use atomic units, with $\hbar = m = e^2 = 1$, throughout this paper.) $(\tau^L + \tau)/2$ has been proposed⁴ as the closest analog of a classical KED. The positivity of τ of Eq. (4) is an extra constraint that makes it easier to model directly than are other choices for the KED; see also Eqs. (9) and (10) below.

While a generalized gradient approximation (GGA) uses only n and ∇n , a meta-GGA (MGGA), such as the accurate nonempirical Tao-Perdew-Staroverov-Scuseria⁵ (TPSS) density functional for the exchange-correlation energy, is constructed from local ingredients $n(\mathbf{r})$, $\nabla n(\mathbf{r})$, and $\tau(\mathbf{r})$. In this work, we will present evidence that $\tau(\mathbf{r})$ and $\nabla^2 n(\mathbf{r})$ can carry essentially the same information beyond that carried by $n(\mathbf{r})$ and $\nabla n(\mathbf{r})$. To do so, and to make an improved semilocal density functional for T_s , we shall construct a Laplacian-level meta-GGA for $\tau(\mathbf{r})$. Our semilocal functional recovers the fourth-order gradient expansion (GE4) KED for a slowly varying density and the von Weizsäcker KED for a rapidly varying density.

The gradient expansion, which becomes exact for densities that vary slowly over space,^{6 is 7}

$$\tau = \tau^{(0)} F_s(p, q, \dots), \quad (5)$$

with

$$F_s = \sum_{n=0}^{\infty} F_s^{(2n)}, \quad (6)$$

where $p = |\nabla n|^2 / [4(3\pi^2)^{2/3} n^{8/3}]$ and $q = \nabla^2 n / [4(3\pi^2)^{2/3} n^{5/3}]$ are dimensionless derivatives of the density, $\tau^{(0)} = \frac{3}{10} (3\pi^2)^{2/3} n^{5/3}$ is the Thomas-Fermi KED,⁸ and

$F_s^{(2n)}(p, q, \dots)$ is the enhancement factor of the $2n$ th term of the gradient expansion. The zeroth-order enhancement factor is⁸ $F_s^{(0)}=1$, and the second-order one is^{9,10} $F_s^{(2)}=(5/27)p + (20/9)q$. The term linear in q is a key ingredient in our MGGA. Although this term integrates to zero in Eq. (1), it is¹¹ important for the KED. This term also indicates rapidly varying density regimes (e.g., near a nucleus where $q \rightarrow -\infty$ and in the tail of the density where $q \rightarrow \infty$). The fourth-order enhancement factor is¹²

$$F_s^{(4)} = \Delta = (8/81)q^2 - (1/9)pq + (8/243)p^2 \geq 0. \quad (7)$$

This enhancement factor is a simplified expression obtained with Green's theorem [integration by parts in Eq. (1)] under the assumption that $n(\mathbf{r})$ and its gradients vanish as $r \rightarrow \infty$. A full expression for $\tau^{(4)}$, involving derivatives of the density of higher than second order, is given in Ref. 10. Although the integration by parts that leads to Eq. (7) is inappropriate for some nonanalytic densities,¹³ we shall incorporate Eq. (7) into our MGGA. The sixth-order term,¹⁴ even if it provides a useful correction to the fourth-order gradient expansion for the formation energy of a monovacancy in jellium,⁷ diverges for atoms after the integration of Eq. (1) and requires higher derivatives of the density than we would like to use. For later use, we define

$$F_s^{GE4}(p, q) = 1 + (5/27)p + (20/9)q + \Delta. \quad (8)$$

The von Weizsäcker expression¹⁵ [$\tau^W = |\nabla n|^2 / (8n)$] is exact for any one- or two-electron ground state, is accurate in nearly iso-orbital regions, satisfies the exact nuclear cusp condition [$\tau(0) = Z^2 n(0) / 2$, where Z is the nuclear charge],¹⁶ is exact in the $r \rightarrow \infty$ asymptotic region [where the density matrix behaves like Eq. (8) of Ref. 17], and gives a rigorous lower bound^{18–20} on the KED of Eq. (4):

$$\tau^W(\mathbf{r}) \leq \tau(\mathbf{r}), \quad (9)$$

or $F_s^W \leq F_s$. The semilocal bound of Eq. (9) is one of the most important constraints in the construction of our functional. The von Weizsäcker enhancement factor¹⁵

$$F_s^W = (5/3)p \geq 0 \quad (10)$$

is simple, but the von Weizsäcker KE functional gives, in general, very poor approximate atomization kinetic energies (see Table III of Ref. 21), and this has been attributed²² to its strong violation of Eq. (8) of Ref. 22.

Recently Tao *et al.*⁵ have constructed a nonempirical meta-generalized-gradient-approximation for the exchange-correlation energy. This functional, which satisfies as many exact constraints as a meta-GGA can (see Table 1 of Ref. 23, or Ref. 24 for a detailed explanation), provides a good overall description of atoms, molecules, solids, and surfaces.^{23–32} We construct a Laplacian-level TPSS (LL-TPSS) by replacing τ by τ^{MGA} in the TPSS exchange-correlation energy per particle.

Gradient-level functionals for exchange and correlation, first proposed in Ref. 33, have been extensively developed since. Laplacian-level functionals for exchange and correlation have been advocated in Ref. 34 and proposed in Ref. 35. Recent interest in them is driven in part by the observation of

Ref. 36 that $\nabla^2 n$ can be used along with n to mimic some exact exchange-correlation conventional energy densities.

The paper is organized as follows. In Sec. II, we present the KED meta-GGA functional. In Sec. III, we test our functional for several physical systems and models, and further explain its behavior. In Sec. IV, we construct the LL-TPSS exchange-correlation functional, and present numerical and analytic evidence that $\nabla^2 n$ and τ carry essentially the same information beyond that carried by n and ∇n . In Sec. V, we summarize our conclusions.

II. CONSTRUCTION OF A META-GGA KINETIC ENERGY DENSITY

Our meta-GGA for the KED is an interpolation between a modified gradient expansion and the von Weizsäcker expression. There are many ways to satisfy the inequality of Eq. (9), so we will have to rely on empiricism to select one of them.

First, we construct a modified fourth-order gradient expansion enhancement factor

$$F_s^{GE4-M} = F_s^{GE4} / \sqrt{1 + \left[\frac{\Delta}{1 + (5/3)p} \right]^2}, \quad (11)$$

which has the following properties:

- (1) For small p and $|q|$,

$$F_s^{GE4-M} = F_s^{GE4} + O(\Delta^2), \quad (12)$$

so that it recovers the fourth order gradient expansion for a slowly varying density.

- (2) When $|q| \rightarrow \infty$,

$$F_s^{GE4-M} \rightarrow 1 + F_s^W, \quad (13)$$

which is the correct limit for a uniform density perturbed by a small-amplitude, short-wavelength density wave.³⁷ When $p \rightarrow \infty$, $F_s^{GE4-M} \rightarrow F_s^W + o(p^0)$, which is reasonable for other rapid density variations.

(3) The modified enhancement factor of Eq. (11) satisfies a uniform damping property:

$$|F_s^{GE4-M}| < |F_s^{GE4}|. \quad (14)$$

This is desirable because for large p and $|q|$, spuriously large values of $|F_s^{GE4}|$ can arise from truncation of the gradient expansion.

We shall assume that the condition $F_s^{GE4-M} < \sim F_s^W$ indicates the need for $F_s^{MGA} = F_s^W$. Our meta-GGA interpolates between F_s^{GE4-M} and F_s^W . The smooth interpolating function is

$$f_{ab}(z) = \begin{cases} 0, & z \leq 0 \\ \left[\frac{1 + e^{a(a-z)}}{e^{a/z} + e^{a(a-z)}} \right]^b, & 0 < z < a \\ 1, & z \geq a, \end{cases} \quad (15)$$

where $0 < a \leq 1$ and $b > 0$ are parameters. This function is plotted in Fig. 1. The meta-GGA KED is defined as follows:

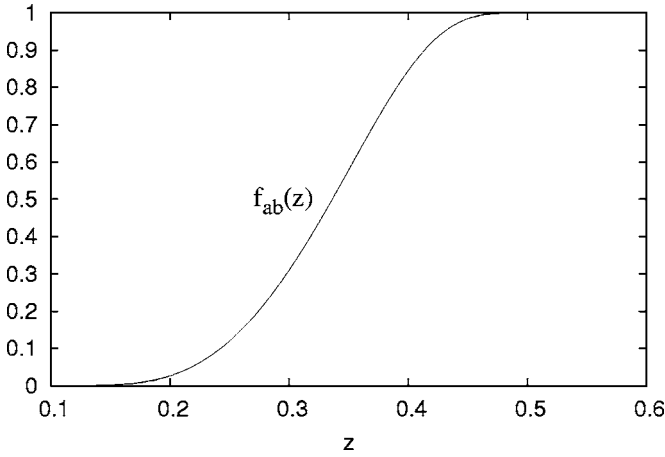


FIG. 1. Interpolating function $f_{ab}(z)$ [see Eq. (15)] versus z for the optimized parameters $a=0.5389$ and $b=3$.

$$\tau^{MGGA} = \tau^{(0)} F_s^{MGGA}(p, q), \quad (16)$$

where

$$F_s^{MGGA} = F_s^W + (F_s^{GE4-M} - F_s^W) f_{ab}(F_s^{GE4-M} - F_s^W). \quad (17)$$

When $f_{ab}=1$, i.e., when $F_s^{GE4-M} > F_s^W + a$, Eq. (17) makes $F_s^{MGGA} = F_s^{GE4-M}$. When $f_{ab}=0$, i.e., when $F_s^{GE4-M} < F_s^W$, Eq. (17) makes $F_s^{MGGA} = F_s^W$. In between, F_s^{MGGA} is an interpolation between F_s^{GE4-M} and F_s^W . Our positive meta-GGA KED keeps all the correct features of τ^{GE4-M} , tends to be exact in iso-orbital regions, and satisfies the important constraint of Eq. (9):

$$F_s^{MGGA} \geq F_s^W. \quad (18)$$

The meta-GGA depends on the empirical parameters a and b . These parameters were found numerically by minimizing the following expression:

$$\begin{aligned} \text{Error} = & \frac{1}{2}(\text{mare atoms}) + \frac{1}{4}(\text{mare clusters}) \\ & + \frac{1}{4}[\text{mare LDM}(N=8)], \end{aligned} \quad (19)$$

where ‘‘mare atoms’’ is the mean absolute relative error (mare) of the integrated kinetic energy of 50 atoms and ions, ‘‘mare clusters’’ is the mare of the KE of $2e^-$, $8e^-$, $18e^-$, $20e^-$, $34e^-$, $40e^-$, $58e^-$, $92e^-$, and $106e^-$ neutral spherical jellium clusters (with bulk parameter $r_s=3.93$, which corresponds to Na), and ‘‘mare LDM($N=8$)’’ is the mare of the KE of $N=8$ jellium spheres for $r_s=2, 4$, and 6 , calculated in the liquid drop model (LDM),

$$T_s^{LDM} = (3/10)k_F^2 N + \sigma_s N^{2/3} 4\pi r_s^2, \quad (20)$$

where $k_F=(3\pi^2 n)^{1/3}$ is the Fermi wave vector, $r_s=(3/4\pi n)^{1/3}$ is the radius of a sphere which contains, on average, one electron, n is the bulk density, and σ_s is the surface KE. The ‘‘exact’’ LDM value is one computed with the exact σ_s . Because the relative errors of surface kinetic energies are much larger than those of the atoms and spherical jellium clusters, we use the LDM approach for calculating the jellium surface KE errors; LDM gives mare comparable to that of atoms and clusters (see Table I). The densities

TABLE I. Mean absolute relative error (mare) of integrated kinetic energies of 50 atoms and ions, of neutral spherical jellium Na clusters ($2e^-$, $8e^-$, $18e^-$, $20e^-$, $34e^-$, $40e^-$, $58e^-$, $92e^-$, and $106e^-$) and of jellium surfaces (with $r_s=2$, $r_s=4$, and $r_s=6$) incorporated into the liquid drop model (LDM) for a jellium sphere with $N=8$ electrons [see Eq. (20)]. The atoms and ions are H, He, Be^{+2} , Be, Be^{+1} , Li, Li^{+1} , Ne, Ne^{+8} , Ne^{+7} , Ne^{+6} , Ar, Ar^{+16} , Ar^{+15} , Ar^{+14} , Ar^{+8} , Ar^{+6} , Zn, Zn^{+28} , Zn^{+20} , Zn^{+18} , Zn^{+12} , Kr, Kr^{+34} , Kr^{+26} , Kr^{+24} , Kr^{+18} , Xe, C^{+4} , C^{+3} , C^{+2} , N^{+5} , N^{+4} , N^{+3} , B^{+1} , B^{+3} , B^{+2} , O^{+1} , O^{+6} , O^{+5} , O^{+4} , Cu, Cu^{+27} , Cu^{+26} , Cu^{+25} , Cu^{+19} , Cu^{+17} , Cu^{+11} , Cu^{+1} and N.

	$T_s^{(0)}$	$T_s^{(0)}+T_s^{(2)}$	$T_s^{(0)}+T_s^{(2)}+T_s^{(4)}$	T_s^{MGGA}
mare atoms	0.0842	0.0112	0.0251	0.0139
mare clusters	0.0439	0.0099	0.0176	0.0245
mare LDM ($N=8$)	0.0810	0.0330	0.0170	0.0247
Error [Eq. (19)]	0.0733	0.0163	0.0212	0.0193

and orbitals we use are analytic Hartree-Fock³⁸ for atoms and ions and numerical Kohn-Sham for clusters and surfaces (with the local-density approximation for the exchange-correlation potential).

In the process of optimization, we observed that the mare decreases very slowly when the parameter $b > 3$ increases, but large values of b deteriorate the KED. So, we chose the following set of parameters: $a=0.5389$ and $b=3$. As we can see in Table I, this set of parameters gives an accuracy close to (but better than) that of the fourth-order gradient expansion.

In Fig. 1, we plot the interpolating function $f_{ab}(z)$ using our choice for the parameters. Near a nucleus, there is a large region where $F_s^{GE4} < 0$ and thus $F_s^{GE4-M} < 0$, making $f_{ab}=0$ and $F_s^{MGGA} = F_s^W$ the correct behavior. (Nevertheless, as $r \rightarrow 0$ and $q \rightarrow -\infty$, $F_s^{GE4-M} \rightarrow 1 + F_s^W$, making $f_{ab} \rightarrow 1$ and $F_s^{MGGA} \rightarrow 1 + F_s^W \approx 1.24$, which is at least positive and finite.) In the $r \rightarrow \infty$ asymptotic region, where $p \approx q \rightarrow \infty$, $F_s^{GE4-M} \rightarrow F_s^W$, making $f_{ab} \rightarrow 0$ and $F_s^{MGGA} \rightarrow F_s^W$ the correct limit. In the slowly varying limit, where p and q are small, $f_{ab}(z) \rightarrow 1$, so meta-GGA recovers the fourth-order gradient expansion. In Fig. 2, we plot the meta-GGA enhancement factor versus $s = \sqrt{p}$ for different values of q . We observe an orderly behavior of F_s^{MGGA} for p and q in the range appropriate to physical densities. For the integrated KE, our meta-GGA is size consistent and satisfies the uniform-scaling relation³⁹ and the spin-scaling relation.³ The meta-GGA nonuniform-scaling behavior is investigated in Sec. III.

III. RESULTS: KINETIC ENERGY AND ITS DENSITY

In Figs. 3 and 4, we plot the integrand of the KE, $4\pi r^2 \tau$, versus radial distance from the nucleus for the He and Ne atoms. The KED of the fourth-order gradient expansion, τ^{GE4} , is negative near the nucleus and is not a good approximation for τ . The meta-GGA KE integrand is much improved near the nucleus, and everywhere follows very nicely the exact behavior.

Let us consider an ion model with ten electrons which occupy the first hydrogenic orbitals and with a nuclear

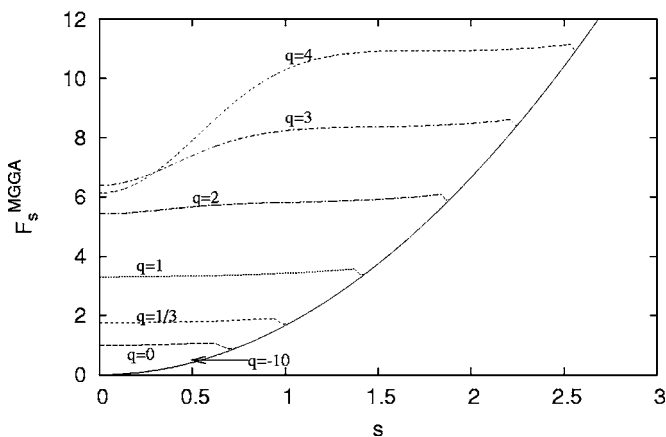


FIG. 2. Enhancement factor $F_s^{MGGA}(p, q)$ versus reduced gradient $s = \sqrt{p}$ for several values of the reduced Laplacian q ($-10, 0, 1/3, 1, 2, 3,$ and 4). The parabolic asymptote is F_s^W .

charge $Z=92$. In such a closed-shell system, the KED is determined by the density of the s electrons alone.^{40,41} In Fig. 5, we show the exact and the meta-GGA kinetic energy densities for this system (for the s electrons and for the whole system, separately).

The KED of the one-electron Gaussian density is shown in Fig. 6. This system does not have a cusp near the center ($r=0$, where $p=0$ and $q \approx -0.5$) and, in this sense, it is an important test for our meta-GGA, which we find to be as accurate here as it is for the He atom.

The Hooke's atom is a simple system of two interacting electrons in a harmonic potential. For this system, the exact KED is the von Weizsäcker one. The correlated wave function and its density can be calculated exactly⁴² for special values of the spring constant k . The low-correlation case⁴³ corresponds to $k=0.25$ a.u., and the high-correlation case⁴⁴ to $k=3.6 \times 10^{-6}$ a.u. A modeled density very similar to the exact Hooke's atom density (with $k=3.6 \times 10^{-6}$ a.u.) is

$$n(r) = A(1 + BCr^2)e^{-Cr^2}, \quad (21)$$

where $A=0.67 \times 10^{-6}$ a.u., $B=11$ a.u., and $C=0.001\,021\,2$ a.u. Applying uniform scaling $n(\mathbf{r}) \rightarrow \gamma^3 n(\gamma\mathbf{r})$

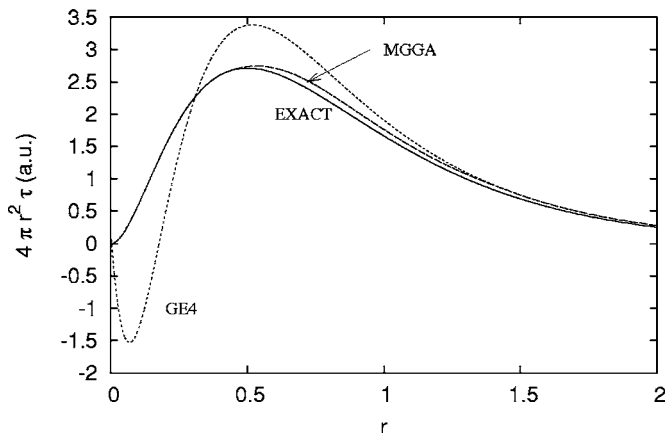


FIG. 3. KE integrand $4\pi r^2 \tau$ versus radial distance r for the He atom. The integral under the curve is the KE for the helium atom: exact, 2.862 a.u.; meta-GGA, 2.993 a.u.; and GE4, 2.963 a.u.

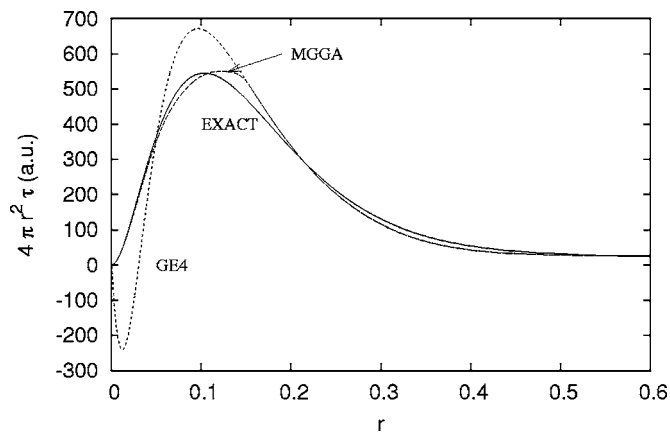


FIG. 4. KE integrand $4\pi r^2 \tau$ versus radial distance r for the Ne atom. The integral under the curve is the KE for the neon atom: exact, 128.546 a.u.; meta-GGA, 129.312 a.u.; and GE4, 129.749 a.u.

$=n_\gamma(\mathbf{r})$, we define the following scaled density:

$$n_\gamma(r) = 0.021\,45(1 + 10.5r^2)e^{-r^2}, \quad (22)$$

with $\gamma=31.753$. In Fig. 7, we show the exact, meta-GGA and fourth-order gradient expansion KE integrands for the pseudo-Hooke's atom [using the scaled density given in Eq. (22)] in the high-correlation case. The region near the nucleus of the pseudo-Hooke's atom is unusual because there strong correlation creates a deep "hole" in the density: q decreases smoothly with increasing r (from 19.29 at $r=0$ to ≈ 0 at $r=0.68$), and p increases slowly with increasing r (from 0 at $r=0$ to a peak value of 1.829 at $r=0.233$). This region cannot be described accurately by the meta-GGA, as we can see in Fig. 7. Near $r=1$, where $p \approx 0$ and $q \approx -0.495$, the KED meta-GGA recovers the exact behavior.

Figures 7 and 8 show how our τ^{MGGA} can sometimes fail to recognize iso-orbital regions where $\tau = \tau^W$. For the $2e^-$ jellium cluster between $r=0.1$ and $r=1$, where p increases very slowly with increasing r (from $p=0.0016$ at $r=0.1$ to

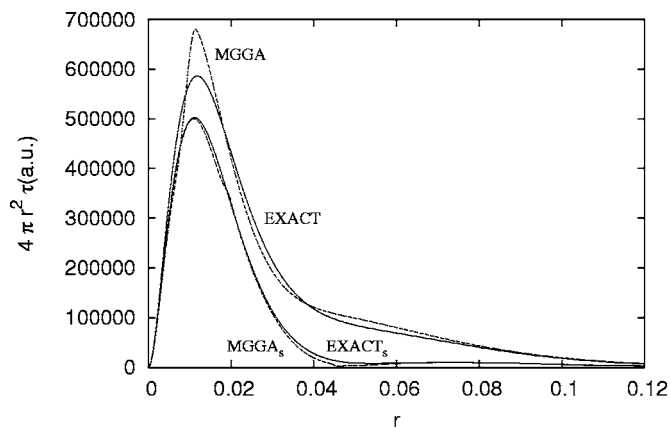


FIG. 5. KE integrand $4\pi r^2 \tau$ versus radial distance r for the ten-electron (hydrogenic orbitals) ion with nuclear charge $Z=92$. The curves $EXACT_s$ and $MGGA_s$ show the contribution of the four s electrons (see Ref. 40).

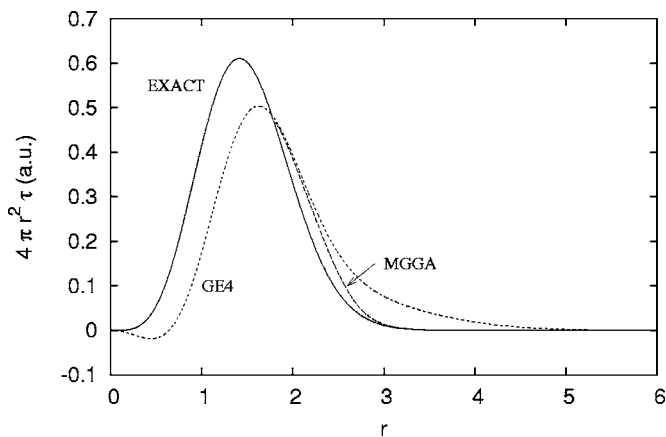


FIG. 6. KE integrand $4\pi r^2 \tau$ versus radial distance r for the one-electron Gaussian density. The integral under the curve is the kinetic energy: exact, 0.750 a.u.; meta-GGA, 0.778 a.u.; and GE4, 0.865 a.u.

$p=0.015$ at $r=1$) and $q=-0.29$, the meta-GGA functional switches from the fourth-order gradient expansion to the exact behavior due to the construction of the interpolating function f_{ab} . This feature is important for molecules, because a similar case arises at the center of a diatomic molecule X_2 .

In Fig. 9, we plot the KED τ versus the scaled distance ζ for the Airy gas, which is the simplest model of an edge electron gas.⁴⁵ In this model, the noninteracting electrons see a linear potential. In the tail of the density, the KED meta-GGA becomes exact (see Fig. 9) as we mentioned in Sec. II. At least two orbital-free kinetic energy functionals have been based upon the Airy gas model. In Ref. 46, the kinetic energy density of the Airy gas is transferred to other systems in a local Airy gas approximation, which seems accurate for jellium surfaces but makes τ diverge at nuclei. In Ref. 47, a density functional is constructed for the linear potential; it has an unphysically rapid oscillation⁴⁸ in its correction to $\tau^{(0)}$ for a slowly varying density.

For a quasi-two-dimensional (quasi-2D) electron gas (quantum well) whose orbitals are those of noninteracting

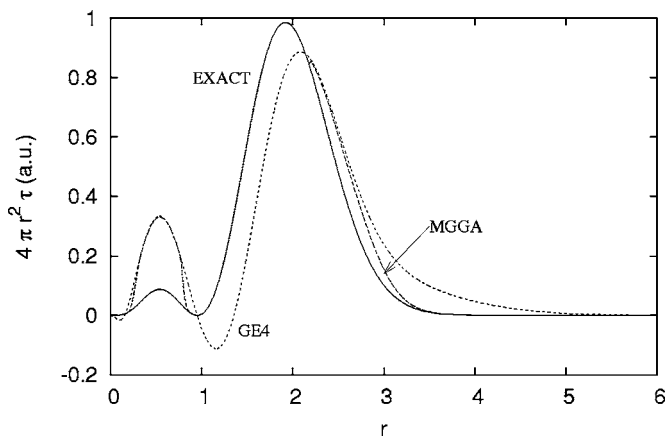


FIG. 7. KE integrand $4\pi r^2 \tau$ versus radial distance r for the pseudo-Hooke's atom in the high-correlation case using the scaled density given in Eq. (22). The integral under the curve is the kinetic energy: exact, 1.115 a.u.; meta-GGA, 1.264 a.u.; and GE4, 1.185 a.u.

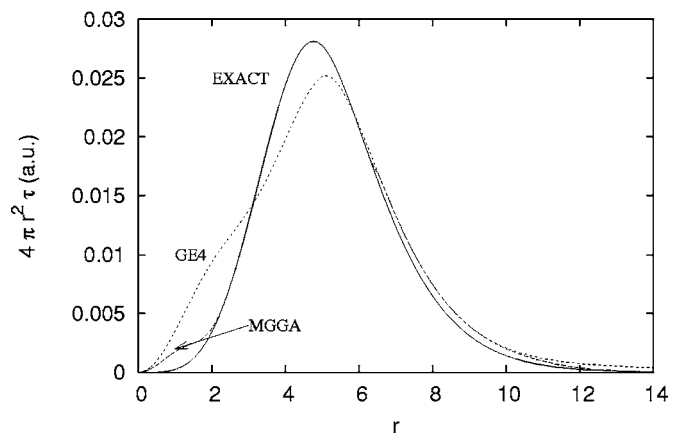


FIG. 8. KE integrand $4\pi r^2 \tau$ versus radial distance r for the $2e^-$ Na jellium spherical cluster. The integral under the curve is the kinetic energy: exact, 0.114 a.u.; meta-CGA, 0.120 a.u.; and GE4, 0.124 a.u.

electrons confined by infinite barriers,⁴⁹ the exact KE per electron can be calculated analytically and has the following simple expression:

$$\frac{T_s}{N} = \frac{\pi^2}{2L^2} + \frac{(k_F^{2D})^2}{4}, \quad (23)$$

where L is the width of the quantum well, $k_F^{2D} = \sqrt{2}/r_s^{2D}$ is the two-dimensional Fermi wave vector, and r_s^{2D} is the radius of the circle that contains, on average, one electron of the quasi-two-dimensional gas. Figure 10 is for the electron gas at $r_s^{2D}=4$. $T_s^{(4)}$ diverges due to the infinite barriers, so it is not shown in the figure. As we can see, the KED meta-GGA functional solves this nonuniform-scaling problem almost exactly.

The nonuniform-scaling inequality⁵⁰ is

$$T_s[n_\lambda^x] \leq \lambda^2 T_s^x[n] + T_s^y[n] + T_s^z[n], \quad (24)$$

where λ is a positive scale factor, the nonuniformly scaled density is $n_\lambda^x(x, y, z) = \lambda n(\lambda x, y, z)$, and $T_s^q[n] = (1/2)(\partial T_s[n_\lambda^q]/\partial \lambda)_{\lambda=1}$, where q is x , y , or z . For the von

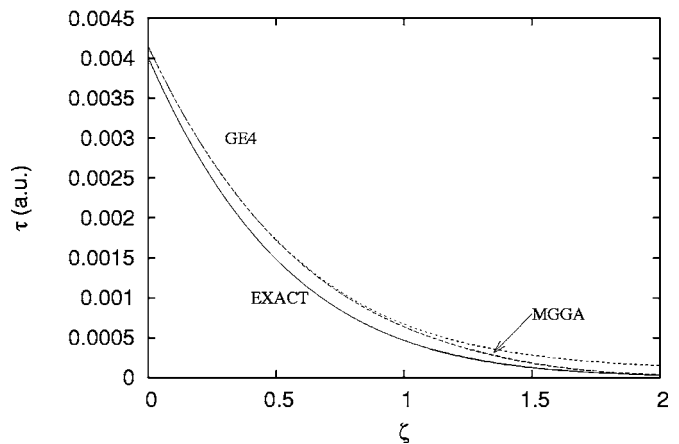


FIG. 9. Kinetic energy density versus Airy scaled distance (Ref. 46) for the Airy gas. The exact KED is given by Eq. (11) of Ref. 46.

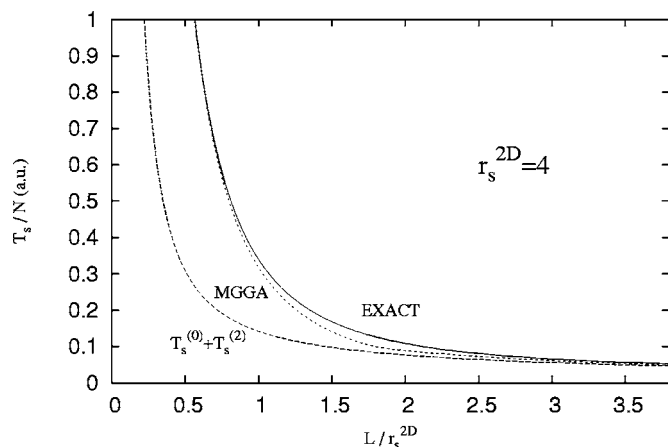


FIG. 10. Integrated kinetic energy per electron versus L/r_s^{2D} for a quasi-2D electron gas in the infinite barrier model. The exact curve is given by Eq. (23). r_s^{2D} is the areal density parameter of the quasi-2D electron gas and L is the width of the quantum well ($L < 3.85r_s^{2D}$, see Ref. 49). Note that $T_s^{(4)}$ diverges here.

Weizsäcker functional, and thus for an exact treatment of the nonuniformly scaled hydrogen atom of density $n_\lambda(r) = (\lambda/\pi)\exp(-2\sqrt{(\lambda x)^2 + y^2 + z^2})$, Eq. (24) becomes an equality.⁵⁰ In Figs. 11 and 12, we show the KE of the nonuniformly scaled hydrogen atom as a function of λ for the prolate case ($\lambda \leq 1$) and oblate case ($\lambda \geq 1$), respectively. As we can see, the meta-GGA KE functional does not satisfy the nonuniform-scaling inequality, but is still very close to the exact behavior. The von Weizsäcker KE is always less than or equal to the meta-GGA functional [see Eq. (18)]. So, the meta-GGA seems to describe the nonuniform-scaling relation with considerable fidelity, a potentially important feature for molecules where the bonding causes nonuniform distortions in the density.

When a molecule at its equilibrium geometry is broken up into separate atoms, the total energy increases and (as suggested by the virial theorem) the kinetic energy decreases. In Table II, we present the atomization kinetic energies for a set of molecules used in Ref. 21. The meta-GGA kinetic energy functional gives the best overall results, but is still not accu-

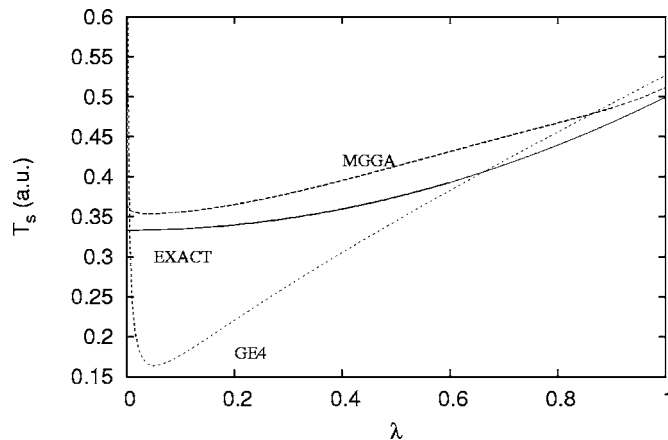


FIG. 11. Integrated KE versus scaling parameter λ for the nonuniformly scaled hydrogen atom in the prolate case.

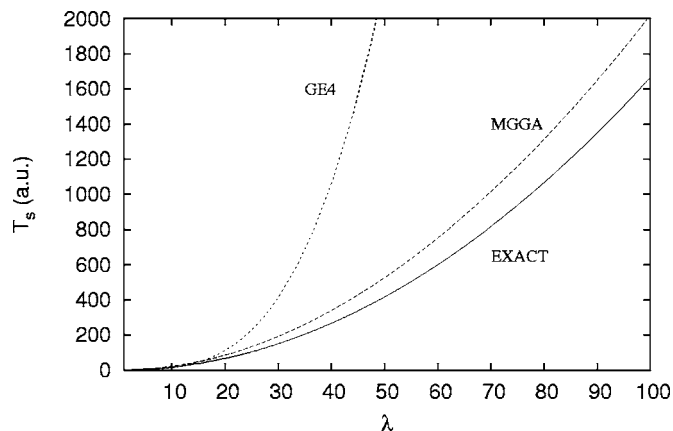


FIG. 12. Integrated KE versus scaling parameter λ for the nonuniformly scaled hydrogen atom in the oblate case.

rate enough for chemical applications. We observe that for NO and O₂ molecules, where the other listed functionals fail badly, the meta-GGA keeps the right sign. (In fact, with the exception of N₂ and F₂, the atomization kinetic energies of the meta-GGA all have the right sign.)

IV. LAPLACIAN-LEVEL META-GGA FOR EXCHANGE-CORRELATION ENERGY

The exchange-correlation meta-GGA uses as ingredients the spin densities and their gradients and the positive Kohn-Sham kinetic energy densities:

TABLE II. Integrated atomization kinetic energy (KE atoms – KE molecule, in a.u.) for a few small molecules. The kinetic energies were calculated using the PROAIMV code with Kohn-Sham orbitals given by the GAUSSIAN2000 code [with the uncontracted 6-311+G(3df,2p) basis set, Becke 1988 exchange functional (Ref. 51), and Perdew-Wang correlation functional (Ref. 52)]. The last line shows the mean absolute errors (mae).

	T_s^{exact}	$T_s^{(0)}$	$T_s^{(0)} + T_s^{(2)}$	$T_s^{(0)} + T_s^{(2)} + T_s^{(4)}$	T_s^{MGGA}
H ₂	-0.150	-0.097	-0.114	-0.119	-0.216
HF	-0.185	-0.305	-0.186	-0.133	-0.352
H ₂ O	-0.304	-0.308	-0.136	-0.057	-0.634
CH ₄	-0.601	-0.737	-0.571	-0.498	-1.036
NH ₃	-0.397	-0.231	-0.060	0.014	-0.477
CO	-0.298	-0.323	-0.085	0.015	-0.458
F ₂	-0.053	0.128	0.282	0.338	0.154
HCN	-0.340	-0.1835	0.079	0.186	-0.328
N ₂	-0.158	0.344	0.565	0.650	0.319
CN	-0.431	-0.215	0.005	0.094	-0.231
NO	-0.268	0.092	0.330	0.422	-0.084
O ₂	-0.100	0.106	0.335	0.431	-0.194
mae		0.177	0.311	0.384	0.201

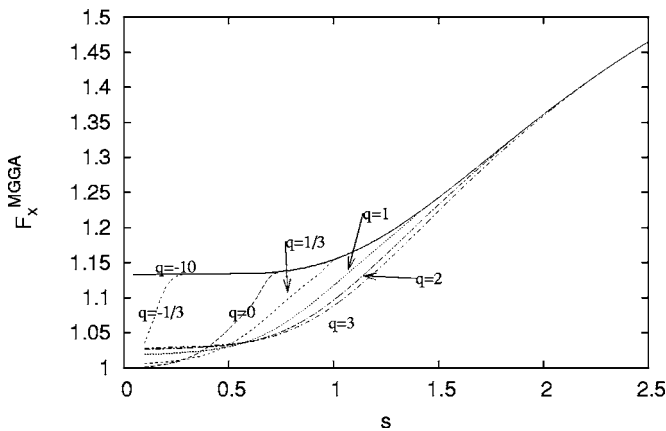


FIG. 13. Exchange enhancement factor $F_x^{LL-TPSS}$ versus reduced gradient $s = \sqrt{p}$ for several values of the reduced Laplacian: $q = -10, -1/3, 0, 1/3, 1, 2, 3$.

$$E_{xc}^{MGGA} = \int d\mathbf{r} n(\mathbf{r}) \epsilon_x^{(0)}(n(\mathbf{r})) \times F_{xc}^{MGGA}(n_\uparrow(\mathbf{r}), n_\downarrow(\mathbf{r}), \nabla n_\uparrow(\mathbf{r}), \nabla n_\downarrow(\mathbf{r}), \tau_\uparrow(\mathbf{r}), \tau_\downarrow(\mathbf{r})), \quad (25)$$

where $\epsilon_x^{(0)}(n) = (-3/4\pi)(3\pi^2 n)^{1/3}$ is the exchange energy per electron of a uniform, spin-unpolarized density n . The local-density approximation (LDA) is recovered for $\nabla n_\uparrow = \nabla n_\downarrow = 0$ and $\tau_\uparrow = \tau_\downarrow^{(0)}$, $\tau_\downarrow = \tau_\uparrow^{(0)}$. Our Laplacian-level noninteracting KED functionals $\tau_\uparrow^{MGGA}(\mathbf{r})$ and $\tau_\downarrow^{MGGA}(\mathbf{r})$ can replace the exact Kohn-Sham kinetic energy densities $\tau_\uparrow(\mathbf{r})$ and $\tau_\downarrow(\mathbf{r})$ in Eq. (25). The resulting LL-MGGA is an explicit density functional, while Eq. (25) is an implicit one. Once an MGGA [Eq. (25)] is programmed, it runs to self-consistency almost as fast as a gradient-level GGA.³⁰ The programming may be simpler for an LL-MGGA, and the construction of the functional derivative is certainly simpler; the LL-MGGA may, however, show spurious oscillations in the functional derivative.

We have constructed in this way the LL-TPSS exchange-correlation meta-GGA.⁵ Like TPSS, LL-TPSS recovers the fourth-order gradient expansion^{5,53} for the exchange energy in the slowly varying limit. Moreover, like TPSS, LL-TPSS has a finite exchange potential at a nucleus. The need for an ingredient beyond n and ∇n (e.g., $\nabla^2 n$) to satisfy this exact constraint was emphasized in Refs. 34 and 44. The nuclear cusp of an atom can be defined by $q \rightarrow -\infty$ and $s \approx 0.376$, so the constraint used in the construction of the TPSS exchange enhancement factor⁵

$$dF_x^{TPSS}(s, z=1)/ds|_{s=0.376} = 0, \quad (26)$$

where $z = \tau(\mathbf{r})/\tau^W(\mathbf{r})$, becomes

$$dF_x^{LL-TPSS}(s, q \rightarrow -\infty)/ds|_{s=0.376} = 0. \quad (27)$$

Such constraints can be satisfied by a Laplacian-level meta-GGA, but not by a GGA (using only n and ∇n).

In Fig. 13, we show the exchange enhancement factor $F_x^{LL-TPSS}$ as a function of the inhomogeneity parameter $s = \sqrt{p}$ for several values of the reduced Laplacian q . The en-

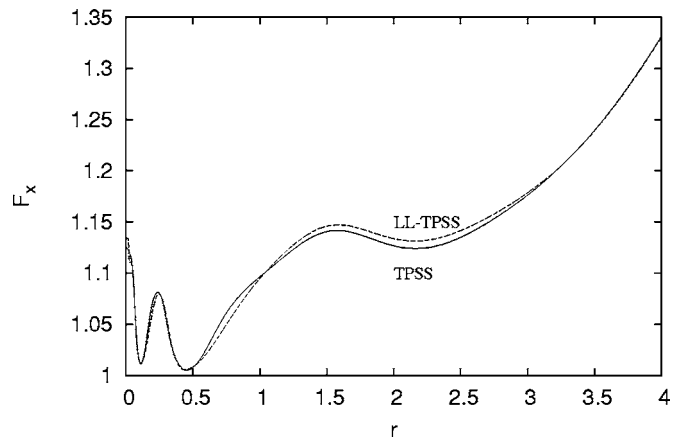


FIG. 14. Exchange enhancement factors $F_x^{LL-TPSS}$ and F_x^{TPSS} versus radial distance r for the Zn atom. $E_x^{TPSS} = -69.798$ a.u. and $E_x^{LL-TPSS} = -69.528$ a.u. Note that $\langle r^{-1} \rangle^{-1}$ is 0.65 for the 3d and 2.26 for the 4s electrons.

hancement factor interpolates in an orderly way between the exact slowly varying limit (for small s and $|q|$) and a rapidly varying limit (for large s) while satisfying Eq. (27).

In Figs. 14 and 15, we compare the TPSS and the LL-TPSS exchange-correlation factors (for exchange and exchange correlation) for the Zn atom, which was also studied in Ref. 24. The LL-TPSS exchange-correlation energies are close to the TPSS values for this and other atoms. (For the H atom, $E_c^{TPSS} = 0$ and $E_c^{LL-TPSS} = -1.537 \times 10^{-6}$; for the other 49 atoms and ions, the error of LL-TPSS with respect to TPSS is 0.001 32 for exchange, 0.0098 for correlation, and 0.001 33 for the combined exchange-correlation energy.)

In Fig. 16, we show that the LL-TPSS exchange functional, like the TPSS, shows a strong enhancement in the 1s region of an atom but is elsewhere not so different from the second-order gradient expansion for exchange, as discussed in Ref. 6.

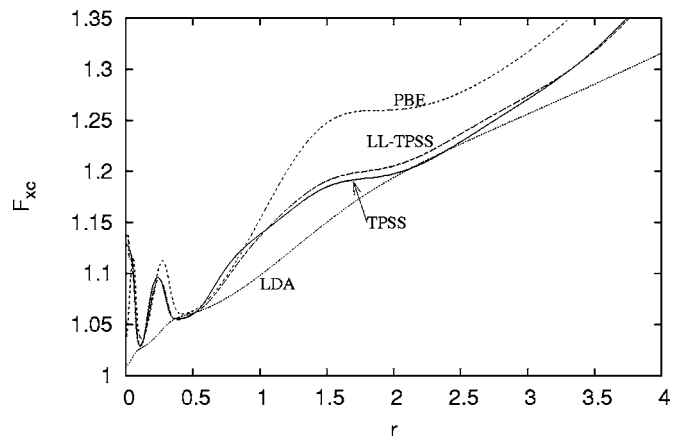


FIG. 15. Exchange-correlation enhancement factors $F_{xc}^{LL-TPSS}$, F_{xc}^{TPSS} , F_{xc}^{PBE} , and F_{xc}^{LDA} versus radial distance r for the Zn atom. $E_{xc}^{TPSS} = -71.208$ a.u., $E_{xc}^{LL-TPSS} = -71.073$ a.u., and $E_{xc}^{PBE} = -70.934$ a.u. Note that $\langle r^{-1} \rangle^{-1}$ is 0.65 for the 3d and 2.26 for the 4s electrons. PBE is the nonempirical GGA of Ref. 54.

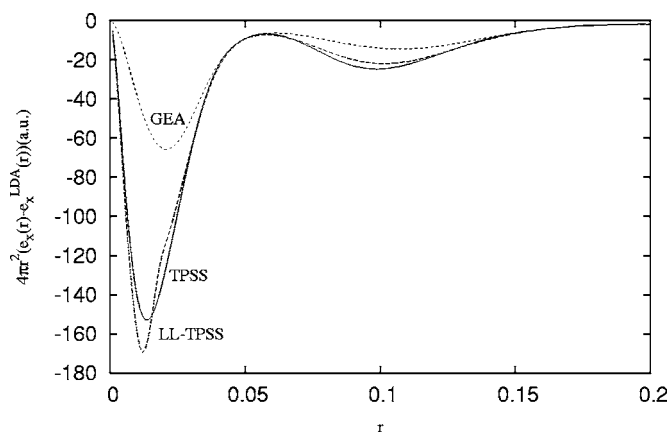


FIG. 16. Deviation (from local-density approximation) of the exchange energy integrand $4\pi r^2 e_x$ versus radial distance r for the Xe atom. GEA is the second-order gradient expansion for exchange. $E_x^{TPSS} = -178.449$ a.u. and $E_x^{LL-TPSS} = -178.240$ a.u.

V. CONCLUSIONS

We have constructed a Laplacian-level kinetic energy density (KED) meta-GGA functional which depends on two empirical parameters. These parameters control an interpolation between a modified fourth-order gradient expansion and the von Weizsäcker expression. This interpolation is designed to respect the exact constraint of Eq. (9). From our tests and results of Sec. III, we conclude that the KED meta-GGA functional is a successful approximation to the positive Kohn-Sham KED.

Our functional uses a simplified expression for the fourth-order gradient expansion¹² of τ . We also tested the meta-GGA with the full fourth-order terms,¹⁰ but did not find a considerable improvement in KED or integrated KE.

We have built a Laplacian-level meta-GGA for exchange and correlation (LL-TPSS) which seems to imitate faithfully

the TPSS (Ref. 5) exchange-correlation meta-GGA. Several constraints of the TPSS meta-GGA are exactly satisfied by the LL-TPSS, but others, such as $E_c=0$ for any one-electron system, are approximately satisfied. It appears to us that $\nabla^2 n$ and τ carry essentially the same information beyond that carried by n and ∇n . Either $\nabla^2 n$ or τ can be and are used to recover the fourth-order gradient expansion of the exchange energy in the slowly varying limit and to make the exchange potential finite at a nucleus.

Integration of our Laplacian-level meta-GGA for the kinetic energy density yields an orbital-free density functional for the kinetic energy that seems to improve upon the fourth-order gradient expansion, especially for rapidly varying densities. We have made all our tests for electron densities constructed from orbitals, and do not know what might be found from a self-consistent solution of the orbital-free Euler equation for the electron density. It was argued in Ref. 55 that KE functionals employing only n and ∇n cannot yield both accurate integrated energies and accurate functional derivatives. We believe that accurate results could be expected in some rapidly varying regions (near nuclei and in density tails) from KE functionals that employ n , ∇n , and $\nabla^2 n$; our specific expressions, however, may encounter a problem due to the sharper features in Fig. 2 (also visible in Fig. 13). It is generally believed that correct quantum density oscillations and shell-structure oscillations can only be found from a fully-nonlocal orbital-free density functional for the kinetic energy.^{56,57}

ACKNOWLEDGMENTS

The authors thank L. M. Almeida for help with the surface code, and Lisa Pollack for early tests such as those of Fig. 10. This work was supported in part by the National Science Foundation under Grants No. DMR 01-35678 and No. DMR 05-01588.

*Present address: Donostia International Physics Center (DIPC), Donostia, Basque Country, Spain.

¹W. Kohn and L. J. Sham, Phys. Rev. **140**, A1133 (1965).

²For a review, see E. V. Ludeña and V. V. Karasiev, in *A Celebration of the Contributions of Robert G. Parr*, edited by K. D. Sen, Reviews of Modern Quantum Chemistry Vol. I (World Scientific, Hackensack, NJ, 2002).

³G. L. Oliver and J. P. Perdew, Phys. Rev. A **20**, 397 (1979).

⁴R. J. Lombard, D. Mas, and S. A. Moszkowski, J. Phys. G **17**, 455 (1991).

⁵J. Tao, J. P. Perdew, V. N. Staroverov, and G. E. Scuseria, Phys. Rev. Lett. **91**, 146401 (2003).

⁶J. P. Perdew, L. A. Constantin, E. Sagvolden, and K. Burke, Phys. Rev. Lett. **97**, 223002 (2006).

⁷Z. Yan, J. P. Perdew, T. Korhonen, and P. Ziesche, Phys. Rev. A **55**, 4601 (1997).

⁸L. H. Thomas, Proc. Cambridge Philos. Soc. **23**, 542 (1926); E. Fermi, Rend. Accad. Naz. Lincei, **6**, 602 (1927).

⁹D. A. Kirzhnits, Sov. Phys. JETP **5**, 64 (1957); *Field Theoretical*

Methods in Many-Body Systems (Pergamon, Oxford, 1967).

¹⁰M. Brack, B. K. Jennings, and Y. H. Chu, Phys. Lett. **65B**, 1 (1976).

¹¹W. Yang, R. G. Parr, and C. Lee, Phys. Rev. A **34**, 4586 (1986).

¹²C. H. Hodges, Can. J. Phys. **51**, 1428 (1973).

¹³J. P. Perdew, V. Sahni, M. K. Harbola, and R. K. Pathak, Phys. Rev. B **34**, 686 (1986).

¹⁴D. R. Murphy, Phys. Rev. A **24**, 1682 (1981).

¹⁵C. F. von Weizsäcker, Z. Phys. **96**, 431 (1935).

¹⁶T. Kato, Commun. Pure Appl. Math. **10**, 151 (1957).

¹⁷M. Ernzerhof, K. Burke, and J. P. Perdew, J. Chem. Phys. **105**, 2798 (1996).

¹⁸T. Hoffmann-Ostenhof and M. Hoffmann-Ostenhof, J. Phys. B **11**, 17 (1978).

¹⁹E. Sagvolden and J. P. Perdew (unpublished).

²⁰S. Kurth, J. P. Perdew, and P. Blaha, Int. J. Quantum Chem. **75**, 889 (1999).

²¹S. S. Iyengar, M. Ernzerhof, S. N. Maximoff, and G. E. Scuseria, Phys. Rev. A **63**, 052508 (2001).

- ²²T. A. Wesolowski, J. Phys. A **36**, 10607 (2003).
- ²³V. N. Staroverov, G. E. Scuseria, J. Tao, and J. P. Perdew, Phys. Rev. B **69**, 075102 (2003).
- ²⁴J. P. Perdew, J. Tao, V. N. Staroverov, and G. E. Scuseria, J. Chem. Phys. **120**, 6898 (2004).
- ²⁵V. N. Staroverov, G. E. Scuseria, J. Tao, and J. P. Perdew, J. Chem. Phys. **119**, 12129 (2003).
- ²⁶G. I. Csonka, A. Ruzsinszky, J. Tao, and J. P. Perdew, Int. J. Quantum Chem. **101**, 506 (2005).
- ²⁷J. Tao and J. P. Perdew, J. Chem. Phys. **122**, 114102 (2005).
- ²⁸J. Tao and J. P. Perdew, Phys. Rev. Lett. **95**, 196403 (2005).
- ²⁹A. Ruzsinszky, J. P. Perdew, and G. I. Csonka, J. Phys. Chem. A **109**, 11006 (2005); **109**, 11015 (2005).
- ³⁰F. Furche and J. P. Perdew, J. Chem. Phys. **124**, 044103 (2006).
- ³¹V. N. Staroverov, G. E. Scuseria, J. P. Perdew, J. Tao, and E. R. Davidson, Phys. Rev. A **70**, 012502 (2004).
- ³²L. A. Constantin, J. P. Perdew, and J. Tao, Phys. Rev. B **73**, 205104 (2006).
- ³³F. Herman, J. P. Van Dyke, and I. B. Ortenburger, Phys. Rev. Lett. **22**, 807 (1967).
- ³⁴C. J. Umrigar and X. Gonze, Phys. Rev. A **50**, 3827 (1994).
- ³⁵P. J'emmer and P. J. Knowles, Phys. Rev. A **51**, 3571 (1995).
- ³⁶A. C. Cancio and M. Y. Chou, Phys. Rev. B **74**, 081202(R) (2006).
- ³⁷W. Jones and W. H. Young, J. Phys. C **4**, 1322 (1971).
- ³⁸E. Clementi and C. Roetti, At. Data Nucl. Data Tables **14**, 177 (1974).
- ³⁹M. Levy and J. P. Perdew, Phys. Rev. A **32**, 2010 (1985).
- ⁴⁰I. A. Howard, N. H. March, and V. E. Van Doren, Phys. Rev. A **63**, 062501 (2001).
- ⁴¹N. H. March and R. Santamaria, Phys. Rev. A **38**, 5002 (1988).
- ⁴²M. Taut, Phys. Rev. A **48**, 3561 (1993).
- ⁴³C. Filippi, C. J. Umrigar, and M. Taut, J. Chem. Phys. **100**, 1290 (1994).
- ⁴⁴C. Filippi, X. Gonze, and C. J. Umrigar, in *Recent Developments and Applications of Modern Density Functional Theory*, Theoretical and Computational Chemistry Vol. 4 (Elsevier, New York, 1996), p. 295.
- ⁴⁵W. Kohn and A. E. Mattsson, Phys. Rev. Lett. **81**, 3487 (1998).
- ⁴⁶L. Vitos, B. Johansson, J. Kollar, and H. L. Skriver, Phys. Rev. A **61**, 052511 (2000).
- ⁴⁷R. Baltin, Z. Naturforsch. A **27A**, 1176 (1972).
- ⁴⁸R. M. Dreizler and E. K. U. Gross, *Density Functional Theory* (Springer-Verlag, Berlin, 1990).
- ⁴⁹L. Pollack and J. P. Perdew, J. Phys.: Condens. Matter **12**, 1239 (2000).
- ⁵⁰Hui Ou-Yang and M. Levy, Phys. Rev. A **42**, 155 (1990).
- ⁵¹A. D. Becke, Phys. Rev. A **38**, 3098 (1988).
- ⁵²J. P. Perdew, in *Electronic Structure of Solids '91*, edited by P. Ziesche and H. Eschrig (Akademie-Verlag, Berlin, 1991).
- ⁵³P. S. Svendsen and U. von Barth, Phys. Rev. B **54**, 17402 (1996).
- ⁵⁴J. P. Perdew, K. Burke, and M. Ernzerhof, Phys. Rev. Lett. **77**, 3865 (1996).
- ⁵⁵B. Wang, M. J. Stott, and U. von Barth, Phys. Rev. A **63**, 052501 (2001).
- ⁵⁶For a review, see Y. A. Wang and E. A. Carter, in *Theoretical Methods in Condensed Phase Chemistry*, edited by S. D. Schwartz, Theoretical Methods in Chemistry and Physics (Kluwer, Dordrecht, 2000).
- ⁵⁷X. Blanc and E. Cancès, J. Phys. Chem. **122**, 214106 (2005).